11th International Conference on Vibration Problems
Z. Dimitrovová *et.al.* (eds.)
Lisbon, Portugal, 9–12 September 2013

COMPOSITE MATERIAL WITH NEGATIVE STIFFNESS INCLUSION FOR VIBRATION DAMPING: THE EFFECT OF A NONLINEAR BISTABLE ELEMENT

Jan Heczko[1], **Zuzana Dimitrovová***[2], **Hélder C. Rodrigues**[3]

[1]Department of Mechanics, Faculty of Applied Sciences, University of West Bohemia, Pilsen
jheczko@kme.zcu.cz

[2]Department of Civil Engineering, Faculdade de Ciências e Technologia, Universidade Nova de Lisboa
zdim@fct.unl.pt

[3]Department of Mechanical Engineering, Instituto Superior Técnico, Technical University of Lisbon
hcr@ist.utl.pt

Keywords: negative stiffness, nonlinear bistable element, vibration control

Abstract. *This work deals with a one-dimensional mechanical system that contains pre-compressed spring elements whereby exhibiting negative stiffness in certain region. Nonlinearity of the pre-compressed elements is the main concern here. Stationary points and their stability with respect to pre-compression and stiffness of a stabilizing element are investigated. The time domain response to harmonic kinematical loading as well as to harmonic force are computed numerically and compared. Steady state is computed for various combinations of parameters and the results are interpreted in view of using the system in passive vibration damping.*

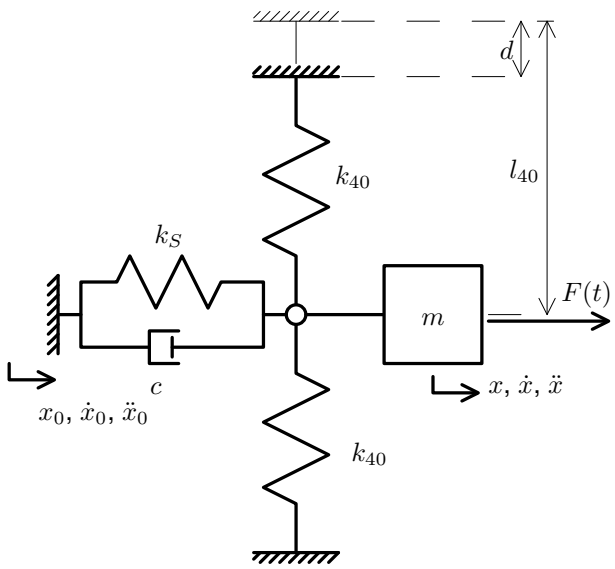

Figure 1: Configuration of the kinematically or force driven 1D system. The prestressed elements, k_{40}, are placed symmetrically.

1 Introduction

Mechanical systems with negative-stiffness elements have been shown to posses the ability of reaching extremal properties, such as stiffness or vibration damping.

The idea of using negative-stiffness elements for passive vibration damping was presented for example in [1] and is used in manufacturing vibration isolating devices. The idea of designing a material with similar properties gained attention in recent years, see e.g. [2] or [5]. Also attempts were made to incorporate a bistable structure into a material to achieve the desired vibration damping behavior [3, 4]

A model considering nonlinearity of the bistable element is derived in [6] but it was not examined in the view of the effects of nonlinearity. A finite strain continuum model of a material is presented in [7]. It is also remarked there that nonlinearity might have positive influence on stability.

The goal of the present paper is to investigate mechanical behavior of a simple one-dimensional system considering nonlinearity of the bistable element that provides negative stiffness. The topology of the system is chosen similar to the mechanism experimentally tested in [8].

2 Model

The system that was investigated is schematically depicted in Fig. 1. It consists of two pre-compressed spring elements, k_{40}, a stabilizing spring element, k_S, a viscous damping element, c, and mass, m. The original length of k_{40} is l_{40} and the amount of pre-compression is denoted d. The motion of the system was investigated only in the direction perpendicular to the k_{40} elements.

Two variants of excitation were considered: (i) kinematic loading, prescribed as time-dependent displacement if the basis, $x_0(t)$, and (ii) force, $F(t)$.

Unless stated otherwise, prescribed values of the parameters of the model were: $m = 1\,\mathrm{kg}$, $c = 0.1\,\mathrm{Nm^{-1}s}$, $l_{40} = 1\,\mathrm{m}$, $d = 0.01\,\mathrm{m}$, $k_{40} = 1\,\mathrm{N/m}$, $k_S = 0.02\,\mathrm{N/m}$. As will be shown in the next section, system with these values of parameters has three stationary points and the origin is unstable.

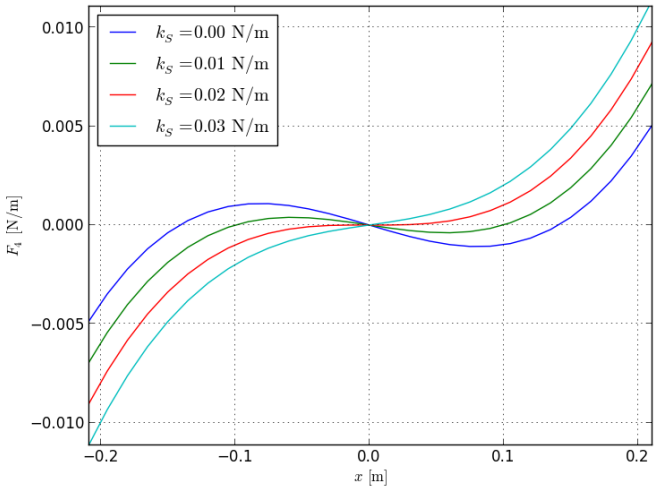

Figure 2: The elastic force, F_4, as a function of displacement for various values of stabilizing stiffness k_S.

The equation of motion of the one-dimensional system described above is

$$m\ddot{x} + c \cdot (\dot{x} - \dot{x}_0) + \underbrace{\left(k_S + 2k_{40}\left(1 - \frac{l_{40}}{\sqrt{(x - x_0)^2 + (l_{40} - d)^2}}\right)\right) \cdot (x - x_0)}_{F_4} = F(t). \quad (1)$$

Figure 2 shows the force F_4 as a function of displacement (assuming $x_0 \equiv 0$). Negative slope is observable for some values of k_S. Roots of $F_4(x)$ correspond to stationary points of the system; this is the topic of section 3.

Using the substitution $y_1 = x$, $y_2 = \dot{x}$, the motion equation, (1), can be written as a system of first-order equations which is better suitable for numerical solution:

$$\begin{aligned}\dot{y}_1 =& y_2\\ \dot{y}_2 =& \frac{1}{m}\left(F(t) - c \cdot (y_2 - \dot{x}_0) - \left(k_S + 2k_{40}\left(1 - \frac{l_{40}}{\sqrt{(y_1 - x_0)^2 + (l_{40} - d)^2}}\right)\right) \cdot (y_1 - x_0)\right)\end{aligned} \quad (2)$$

3 Stationary points

Considering system (2) in the form $\dot{\mathbf{y}} = \mathbf{f}(\mathbf{y})$ (independent of time, i.e. no loading: $F \equiv 0$ and $x_0 \equiv 0$), the stationary points $\mathbf{y}_S$ are given as a solution of

$$\mathbf{f}(\mathbf{y}_S) = \mathbf{0}. \quad (3)$$

Obvious from the first equation of (2) is that $y_2 = 0$ for all stationary points $\mathbf{y}_S = [y_1, y_2]$. The second equation of (2) becomes

$$\left(k_S + 2k_{40}\left(1 - \frac{l_{40}}{\sqrt{y_1^2 + (l_{40} - d)^2}}\right)\right) \cdot y_1 = 0 \quad (4)$$

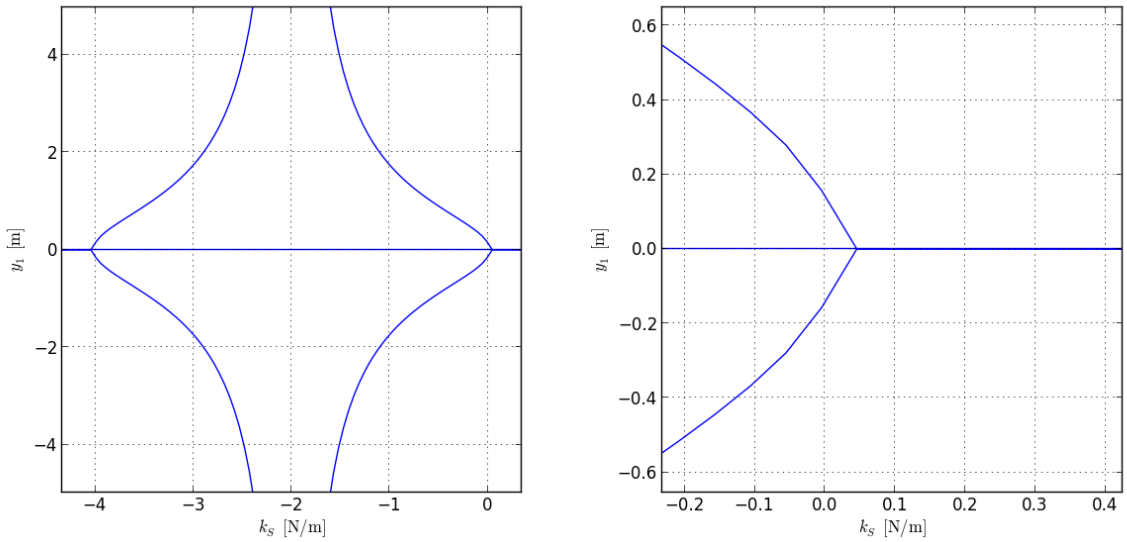

(a) Stationary points (coordinate y_1). (b) Magnified closer to the positive values of k_S.

Figure 3: Stationary points (coordinate y_1), dependence on k_S.

which yields the other component of a stationary point

$$y_1 = 0 \tag{5}$$

and

$$k_S + 2k_{40}\left(1 - \frac{l_{40}}{\sqrt{y_1^2 + (l_{40} - d)^2}}\right) = 0 \tag{6}$$

which yields the components y_1 of two additional stationary points

$$y_1 = \pm\sqrt{\frac{l_{40}^2}{\left(\frac{k_S}{2k_{40}} + 1\right)^2} - (l_{40} - d)^2}. \tag{7}$$

The additional stationary points are present when the following relation is fulfilled:

$$\frac{l_{40}^2}{\left(\frac{k_S}{2k_{40}} + 1\right)^2} - (l_{40} - d)^2 \geq 0. \tag{8}$$

The dependence of coordinate y_1 of the stationary points on k_S is shown in Fig. 3.

To sum up, the stationary points of (2) are ($\mathbf{y}_{Si} = [y_{1i}, y_{2i}]$):

$$\begin{aligned}
\mathbf{y}_{S1} &= [0, 0] \\
\mathbf{y}_{S2} &= \left[\sqrt{\frac{l_{40}^2}{\left(\frac{k_S}{2k_{40}} + 1\right)^2} - (l_{40} - d)^2}, 0\right] \\
\mathbf{y}_{S3} &= \left[-\sqrt{\frac{l_{40}^2}{\left(\frac{k_S}{2k_{40}} + 1\right)^2} - (l_{40} - d)^2}, 0\right]
\end{aligned} \tag{9}$$

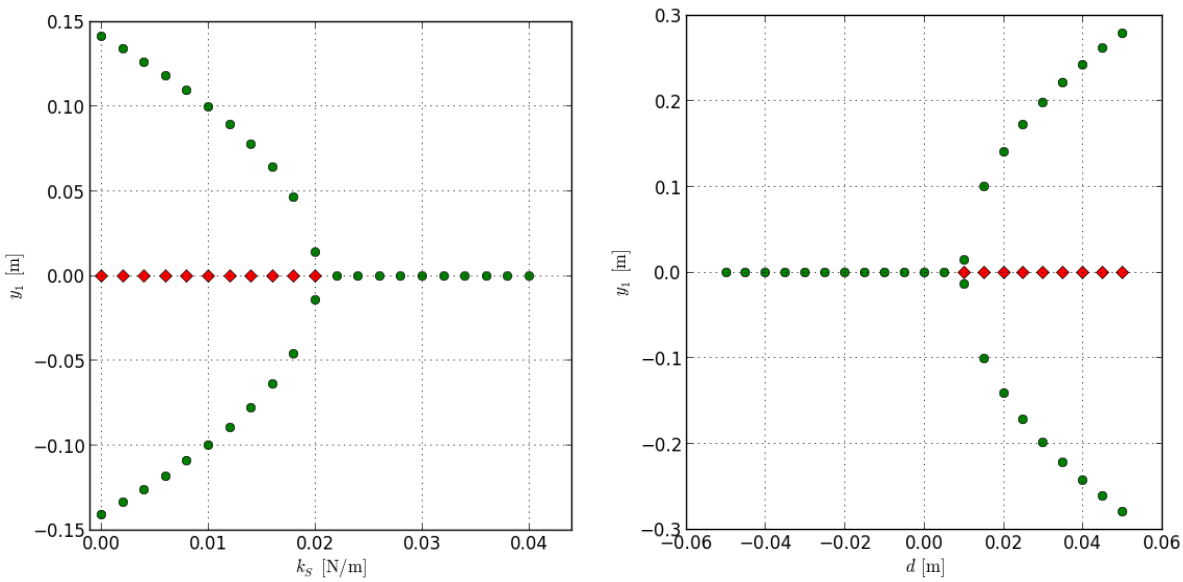

Figure 4: Stationary points (the y_1 coordinate) and their stability for various values of k_S and d; green circles denote stable nodes, red squares denote saddle points.

3.1 Stability of the stationary points

Stability of the stationary points was determined numerically by using eigenvalues of the jacobian matrix of (2) (again with $F \equiv 0$ and $x_0 \equiv 0$):

$$\mathbf{J}(y_1, y_2) = \begin{bmatrix} 0 & 1 \\ \frac{1}{m}\left(k_S - 2k_{40}\left(1 - \frac{l_{40}}{\sqrt{y_1^2+(l_{40}-d)^2}}\right) - \frac{2k_{40}l_{40}y_1^2}{\left(y_1^2+(l_{40}-d)^2\right)^{\frac{3}{2}}}\right) & -\frac{c}{m} \end{bmatrix} \tag{10}$$

Stability of stationary points and dependence on parameters k_S and d is shown in Fig. 4. According to [3], the system should operate between the stable points of the system with $k_S = 0$ to achieve the desired vibration-damping properties.

Phase portraits for different values of k_S are shown in Fig. 5. Phase portraits of kinematically loaded system are shown in Fig. 6.

4 Steady-state response

The steady-state response of a periodically driven system was computed using numeric integration. The method used was, as in all cases of numeric integration mentioned in this work, explicit fifth order Runge-Kutta method as implemented in SciPy python library.

The solution was sought under the assumption that the period of the solution equals the period of loading. Therefore the steady-state-searching procedure consisted in successive solution to initial value problems of the form

$$\begin{aligned} \dot{\mathbf{y}}^i(t) &= \mathbf{f}(\mathbf{y}^i(t), t), \quad t \in \langle 0, T \rangle \\ \mathbf{y}^i(0) &= \mathbf{y}^{i-1}(T) \end{aligned} \tag{11}$$

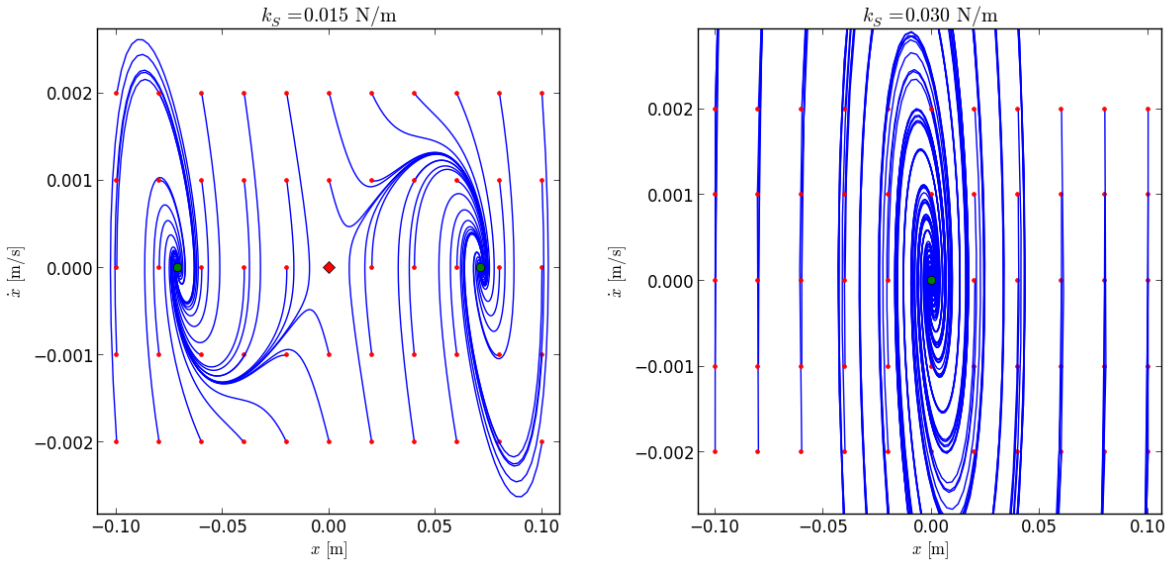

Figure 5: Phase portraits of a free system. Red dots denote the initial conditions, where the trajectories begin. Stability of stationary points: green circle is a stable node, red square a saddle point.

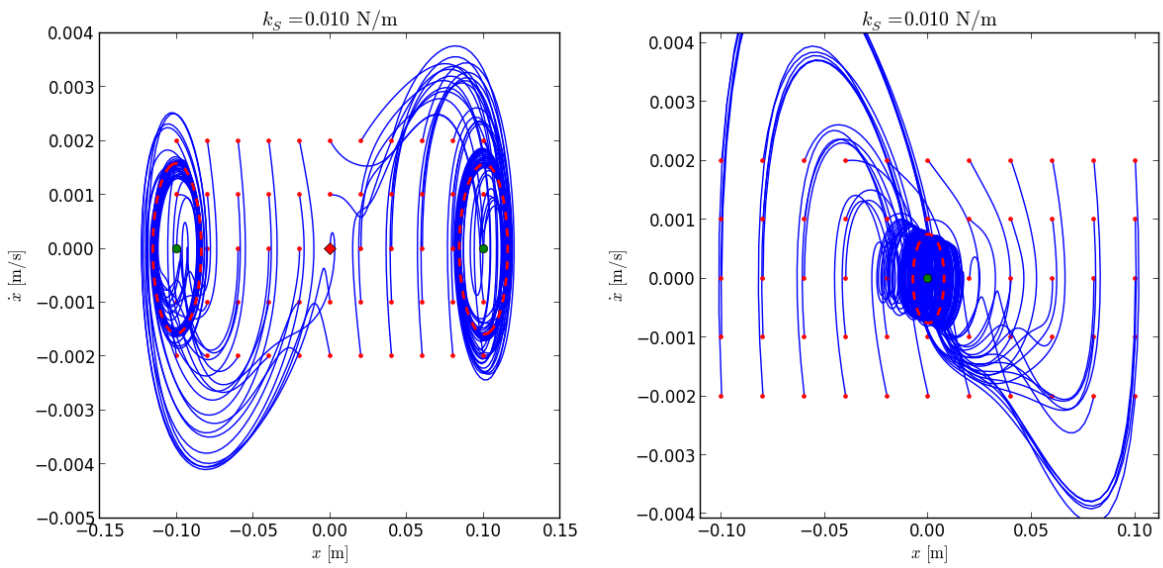

Figure 6: Phase portraits of kinematically loaded system. Dashed red lines represent steady-state trajectories. The prescribed parameters of harmonic loading were in this case: angular frequency $\omega = 0.01\,\mathrm{rad/s}$, amplitude $X_0 = 0.01\,\mathrm{m}$.

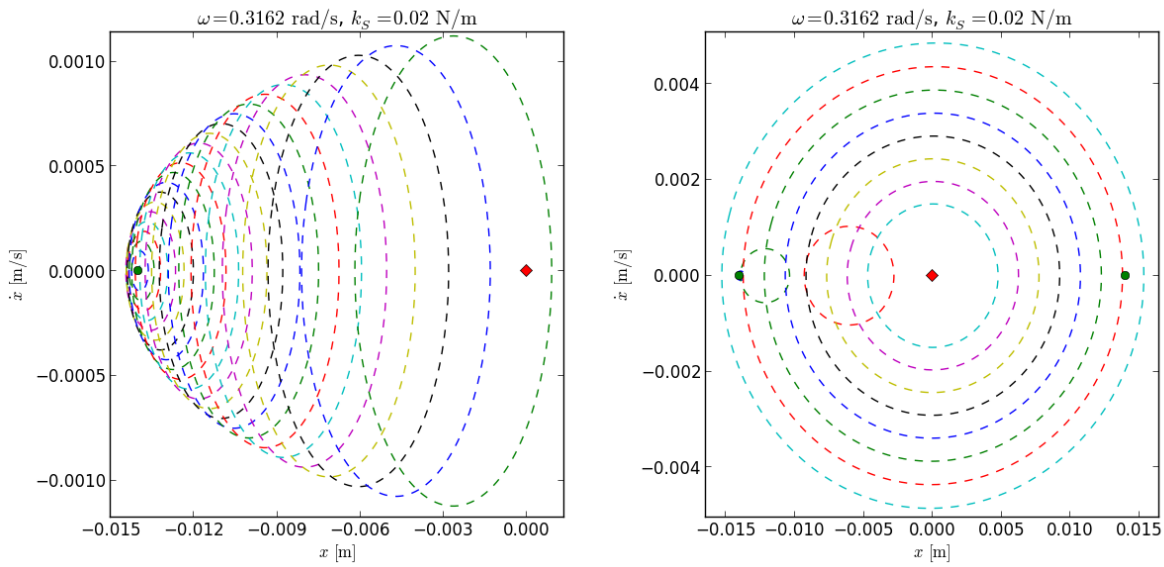

(a) $X_0 \in \langle 0.001\,\mathrm{m}, 0.012\,\mathrm{m}\rangle$ (b) $X_0 \in \langle 0.001\,\mathrm{m}, 0.050\,\mathrm{m}\rangle$

Figure 7: Steady-state paths in phase space (attractors) at driving frequency $\omega = 0.3162\,\mathrm{rad/s}$ for various values of amplitude X_0. The plots are symmetric about the vertical axis, but here only the left-side half of attractors is shown.

with the stopping criterion

$$\sum_{k=1}^{2} \frac{\|\mathbf{y}_k^i - \mathbf{y}_k^{i-1}\|}{Y_k} < \varepsilon \tag{12}$$

for a chosen value of ε (here $\varepsilon = 10^{-8}$). In the above, $\mathbf{y}_k^i$ and $\mathbf{y}_k^i$ stand for the k-th component of response (i.e. displacement, $x = y_1$ or velocity, $\dot{x} = y_2$); the vector $\mathbf{y}_k^i$ contains values at all time instants that have been computed. The amplitude $Y_k = \frac{1}{2}\left(\max\{\mathbf{y}_k^i\} - \min\{\mathbf{y}_k^i\}\right)$. To avoid unacceptably long computations, an additional stopping criterion was used:

$$i > maxiter \tag{13}$$

where $maxiter$ was varied according to the purpose of the computation. For example for plotting the attractors in phase space $maxiter = 50000$ was set but for computing the basins of attraction there was no need for such accuracy therefore only $maxiter = 200$ was set.

4.1 Kinematically loaded system

The kinematic loading was defined as:

$$x_0(t) = X_0 \cdot \cos(\omega \cdot t), \quad F(t) \equiv 0, \tag{14}$$

where the amplitude, X_0, and angular frequency, ω, are chosen parameters.

Figure 7 shows the attractors in phase space. It can be seen that the attractors move toward the origin when amplitude of loading increases. The dependence of attractor position on loading amplitude is captured in Fig. 8. The picture also shows the size of the attractors in the y_1-direction (which is actually twice the amplitude of displacement) and the y_1 coordinate of one of the stationary points. Since certain value of X_0, the attractors are all centered at the origin

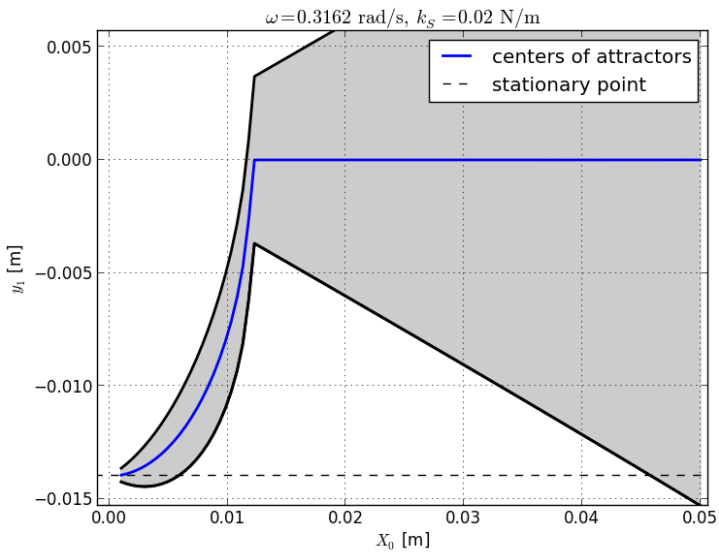

Figure 8: The y_1-position of attractor centers of the kinematically loaded system. The grey area corresponds to the interval that is spanned by the attractor in y_1 direction.

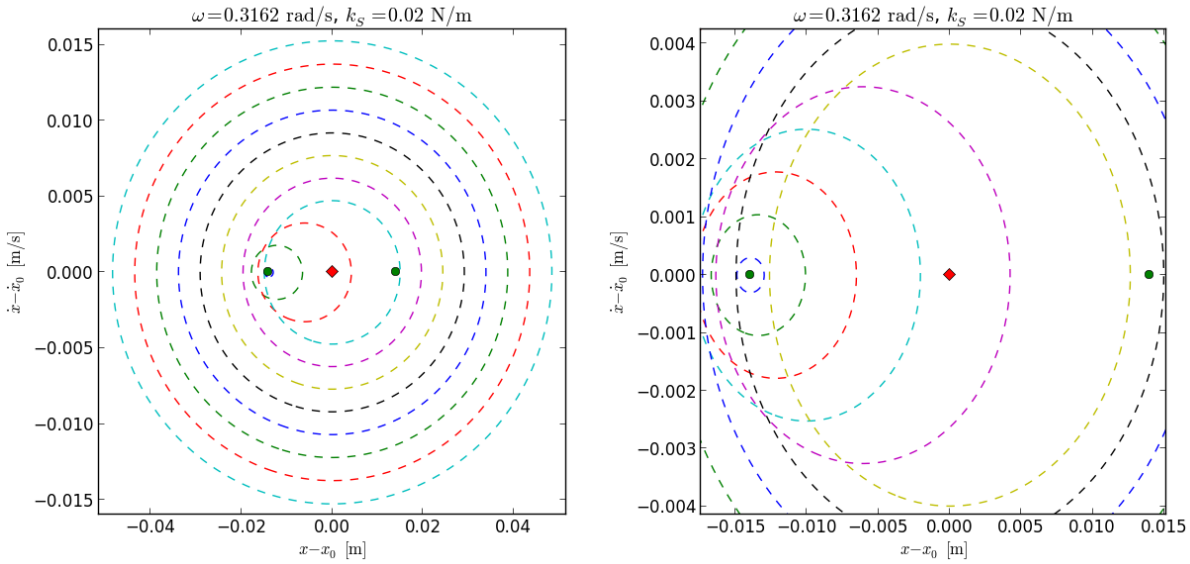

Figure 9: Relative position of the attractors of kinematically loaded system for various values of loading amplitude $X_0 \in \langle 0.001\,\mathrm{m},\ 0.05\,\mathrm{m}\rangle$; below is the central part magnified.

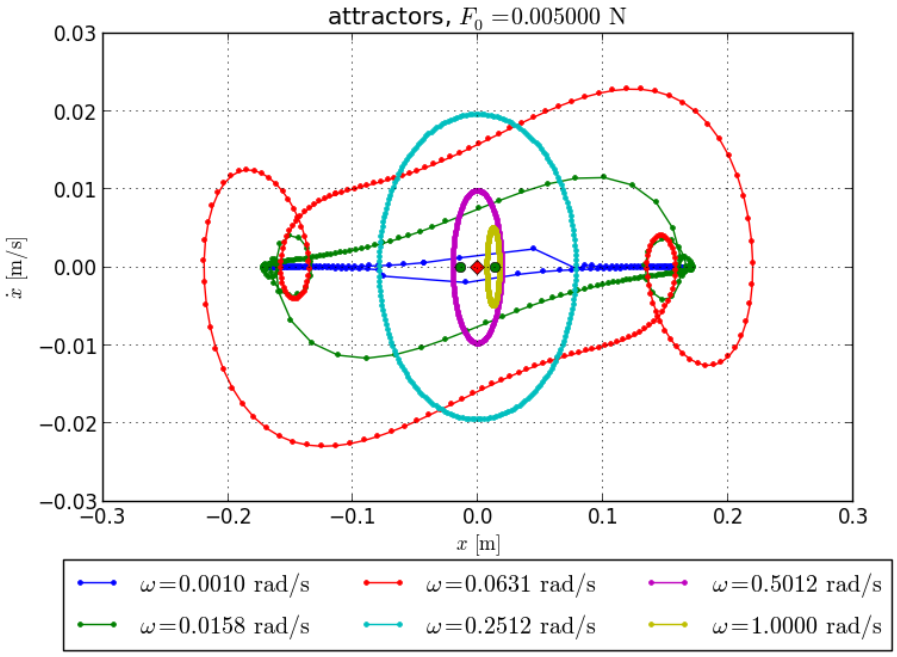

Figure 10: Steady-state paths in phase space (attractors) for various values of driving frequency, ω, and with amplitude fixed $F_0 = 0.005\,\mathrm{N}$.

(which is the unstable stationary point for this combination of parameters).

Attractors in relative coordinates (after subtraction of x_0 and $\dot{x}_0$ are shown in Fig. 9. At least one stationary point lies inside all attractors after this transformation.

4.2 Force-loaded system

The harmonic loading by a force was defined similarly as in the previous section:

$$x_0 \equiv 0, \quad F(t) = F_0 \cdot \sin(\omega t). \tag{15}$$

Figure 10 shows the attractors of a system loaded with harmonic force $F(t) = F_0 \cdot \sin(\omega t)$ for various values of driving frequency ω.

While the attractors in previous section, 4.1, were almost all of elliptic shape, the attractors of a force-loaded system contain small loops. For higher values of excitation frequency, however, the attractors also convert to elliptic shape.

5 Conclusions

The one-dimensional system investigated in this work contains a bistable element. When the nonlinear behavior of this element is respected in computations, there is no need for a stabilizing element since the system is unstable only in a bounded interval. Nevertheless, a condition was derived for the stabilizing stiffness k_S, above which the system has only one stationary point that is stable (eq. (8)).

In the case of kinematically loaded system, there are two stable attractors up to certain loading amplitude value but there is only one attractor centered at the origin for larger magnitudes of loading.

REFERENCES

[1] D. L. Platus, Negative-Stiffness-Mechanism Vibration Isolation Systems, *Proceedings of SPIE, Vibration Control in Microelectronics. Optics, and Metrology*, **1619**, 44 – 54.

[2] R. S. Lakes, Extreme Damping in Composite Materials with a Negative Stiffness Phase, *Physical Review Letters*, **86**(13), 2001.

[3] R. S. Lakes, Extreme damping in compliant composites with a negative-stiffness phase, *Philosophical Magazine Letters*, **81**(2), 95 – 100, 2001.

[4] L. Kashdan, *Evaluation of Negative Stiffness Elements for Enhanced Material Damping Capacity*, master's thesis, 2010.

[5] J. Prasad, A. R. Diaz, Viscoelastic material design with negative stiffness components using topology optimization, *Struct Multidisc Optim*, **38**, 583 –597, 2009

[6] Y. Wang, R. S. Lakes, Negative stiffness-induced extreme viscoelastic mechanical properties: stability and dynamics, *Philosophical Magazine*, **84**(35), 3785 – 3801, 2004.

[7] W. J. Drugan, R. S. Lakes, Dramatically stiffer elastic composite materials due to a negative stiffness phase?, *Journal of the Mechanics and Physics of Solids*, **50**, 979 – 1009, 2002.

[8] L. Kashdan, C. C. Seepersad, M. Haberman, P. S. Wilson, Design, fabrication, and evaluation of negative stiffness elements using SLS, *Rapid Prototyping Journal*, **18**(3), 194 – 200, 2012.